A Hybrid Density Functional Study of O−O Bond Cleavage and Phenyl Ring Hydroxylation for a Biomimetic Non-Heme Iron Complex

ARTICLE *in* INORGANIC CHEMISTRY · JUNE 2004

Impact Factor: 4.76 · DOI: 10.1021/ic035395c · Source: PubMed

3 AUTHORS, INCLUDING:

Tomasz Borowski

Instytut Katalizy i Fizykochemii Powierzchni i…

45 PUBLICATIONS **1,210** CITATIONS

SEE PROFILE

Inorg. Chem. **2004**, *43*, 3277−3291

A Hybrid Density Functional Study of O–O Bond Cleavage and Phenyl Ring Hydroxylation for a Biomimetic Non-Heme Iron Complex

Tomasz Borowski,* Arianna Bassan, and Per E. M. Siegbahn

Department of Physics, Stockholm Center for Physics, Astronomy and Biotechnology, Stockholm University, S-106 91 Stockholm, Sweden

Received December 4, 2003

Density functional calculations using the B3LYP functional have been used to study the reaction mechanism of [Fe(Tp^{Ph2})BF] (Tp^{Ph2} = hydrotris(3,5-diphenylpyrazol-1-yl)borate; BF = benzoylformate) with dioxygen. This mononuclear non-heme iron(II) complex was recently synthesized, and it proved to be the first biomimetic complex reproducing the dioxygenase activity of α-ketoglutarate-dependent enzymes. Moreover, the enthalpy and entropy of activation for this biologically interesting process were derived from kinetic experiments offering a unique possibility for direct comparison of theoretical and experimental data. The results reported here support a mechanism in which oxidative decarboxylation of the keto acid is the rate-limiting step. This oxygen activation process proceeds on the septet potential energy surface through a transition state for a concerted O–O and C–C bond cleavage. In the next step, a high-valent iron–oxo species performs electrophilic attack on the phenyl ring of the Tp^{Ph2} ligand leading to an iron(III)–radical σ-complex. Subsequent proton-coupled electron-transfer yields an iron(II)–phenol intermediate, which can bind dioxygen and reduce it to a superoxide radical. Finally, the protonated superoxide radical leaves the first coordination sphere of the iron(III)–phenolate complex and dismutates to dioxygen and hydrogen peroxide. The calculated activation barrier (enthalpy and entropy) and the overall reaction energy profile agree well with experimental data. A comparison to the enzymatic process, which is suggested to occur on the quintet surface, has been made.

I. Introduction

α-Ketoglutarate (α-KG)-dependent dioxygenases constitute the largest class of mononuclear non-heme iron enzymes whose representatives can be found in plants, animals, and human beings.[1−4] Even though a very broad range of chemical transformations is performed by these enzymes, a common feature is that in all cases the reaction catalyzed is a two-electron oxidation of the primary substrate coupled with an oxidative decarboxylation of the cosubstrate, i.e., α-KG (2-oxo-1,5-pentanedioic acid). Four electrons released in substrate and cosubstrate oxidations are utilized to reduce dioxygen.

Interestingly, besides the broad class of α-KG-dependent dioxygenases, a closely related group of enzymes is currently emerging, and it is termed internal keto acid-dependent dioxygenases. The name originates from the fact that in these enzymes the keto acid plays both the role of primary substrate and of cosubstrate. A representative example is 4-hydroxyphenylpyruvate dioxygenase (4-HPPD), which is an important enzyme involved in tyrosine catabolism.[5] Another member of this group, which was recently identified, is 4-hydroxymandelate synthase (4-HMAS), which plays a key role in biosynthesis of antibiotics from the vancomycin family.[6] The reaction catalyzed by 4-HPPD, see Scheme 1a, involves oxidative decarboxylation of 4-hydroxyphenylpyruvate (HPP) coupled to dioxygen activation. Once dioxygen is activated, the highly reactive iron−oxo species performs phenol ring oxidation, which together with a 1,2-shift of the

* To whom correspondence should be addressed. E-mail: borowski@physto.se. Phone: +46 8 55378703. Fax: +46 8 55378601.

(1) Prescott, A. G.; Lloyd, M. D. *Nat. Prod. Rep.* **2000**, *17*, 367−383.
(2) Schofield, C. J.; Zhang, Z. *Curr. Opin. Struct. Biol.* **1999**, *9*, 722−731.
(3) Solomon, E. S.; Brunold, T. C.; Davis, M. I.; Kemsley, J. N.; Lee, S. K.; Lehnert, N.; Neese, F.; Skulan, A. J.; Yang, Y. S.; Zhou, J. *Chem. Rev.* **2000**, *100*, 235−349.
(4) Bugg, T. D. H. *Tetrahedron* **2003**, *59*, 7075−7101.
(5) Serre, L.; Sailland, A.; Sy, D.; Boudec, P.; Rolland, A.; Pebay-Peyroula, E.; Cohen-Addad, C. *Structure* **1999**, *7*, 977−988.
(6) Choroba, O. W.; Williams, D. H.; Spencer, J. B. *J. Am. Chem. Soc.* **2000**, *122*, 5389−5390.

10.1021/ic035395c CCC: $27.50
Published on Web 04/13/2004

Scheme 1. (a) Proposed Reaction Mechanism for 4-HPPD and (b) Proposed Mechanism for the Biomimetic Reaction of **1**

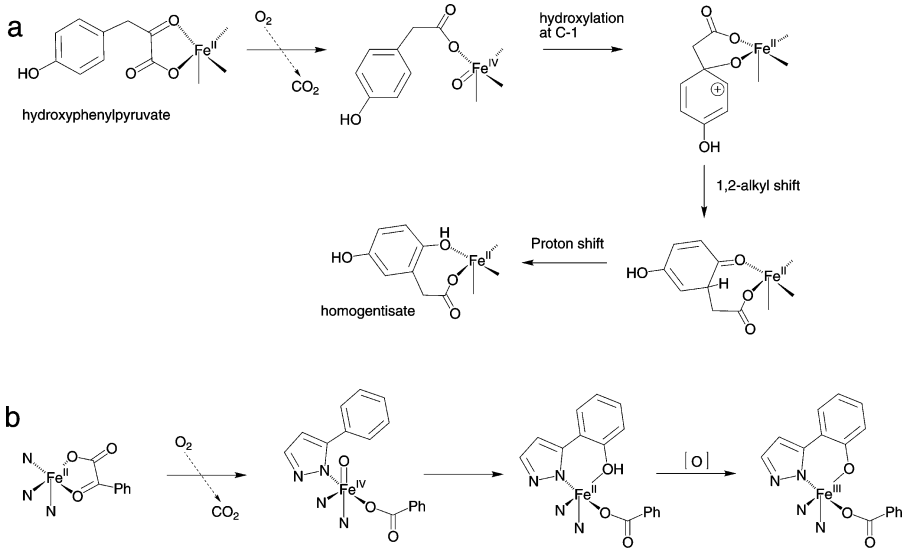

acetic group and proton dislocation leads to the final product, i.e., homogentisate.[4]

In parallel to biochemical studies, research in the area of inorganic complexes, mimicking the catalytic activity of these enzymes, has shed much light on the enzymatic mechanism of keto acid-dependent oxygenases. Comparison of the efficiency of 5- and 6-coordinated model systems demonstrated that the coordinatively unsaturated compounds react with dioxygen much faster, most likely due to the important role of the vacant position in the ferrous ion complex.[7,8] Following this experimental evidence, it was proposed that dioxygen binds to iron and forms a ferric−superoxo species ($Fe^{3+}-O_2^{\bullet-}$) capable of performing a nucleophilic attack on the carbonyl carbon of the α-keto acid.[9,10] Irrespective of the identity of the products of this nucleophilic step, all mechanisms proposed in the literature invoke high-valent iron−oxo species as the most plausible oxidant produced by oxidative decarboxylation of the keto acid.

One series of α-keto acid model complexes was recently studied by Mehn and co-workers.[11,12] The leading compound of this series is [Fe(Tp^{Ph2})BF] (**1**) (Tp^{Ph2} = hydrotris(3,5-diphenylpyrazol-1-yl)borate; BF = benzoylformate), whose crystal structure is presented in Figure 1a. In this complex, iron(II) is coordinated by a tridentate, face-capping Tp^{Ph2} ligand and chelated by benzoylformate. Tp^{Ph2}, which binds to iron in a monoanionic form, is supposed to mimic the 2-His-1-carboxylate facial triad usually found in α-KG-dependent enzymes. The second ligand, BF, is an α-keto acid mimicking α-KG and, at the same time, allowing for introduction of substituents which can tune the electronic properties of the cofactor. This charge-neutral, 5-coordinate complex (**1**) reacts with dioxygen to afford a green product, which was identified as an iron(III)−phenolate complex. In Scheme 1, it can be noticed that the mechanism proposed for this biomimetic reaction (Scheme 1b) resembles the enzymatic process of 4-HPPD (Scheme 1a). In addition, isotope labeling experiments performed for this model complex demonstrated that both oxygen atoms of O_2 are incorporated into the products. One atom is found in the product of decarboxylation, benzoate, while the other is the phenol oxygen in the oxidized ring of the Tp^{Ph2} ligand. Because the biomimetic system successfully reproduces the dioxygenase features of keto acid-dependent enzymes, the steps involving dioxygen activation and subsequent phenyl ring oxidation are likely to be very similar in the two systems. However, after the attack of the iron−oxo species on the phenyl ring, the two reaction paths have to diverge because of the different chemical identity of the final products (see Scheme 1). In the case of the biomimetic system, the iron(II)−phenol complex is oxidized by excess oxygen to the green iron(III)−phenolate product, while in 4-HPPD, carboxymethyl shift and subsequent proton migration lead to the Fe(II)−homogentisate complex. Despite this mechanistic difference, **1** is an excellent model system, coupling decarboxylation of a keto acid with oxidation of the phenyl ring and, therefore, successfully mimicking the chemistry of 4-HPPD.

The detailed kinetic analysis of the reaction between **1** and O_2 showed that this process is first order in either of the reactants.[12] Measurements at different temperatures have provided enthalpy and entropy of activation for the biomimetic reaction. Notably, since no intermediate was detected in the course of the reaction, it is believed that the steps up to the oxidative decarboxylation of the keto acid control the overall rate of the reaction, and therefore, the kinetic and thermodynamic data relate to them.

(7) Chiou, Y. M.; Que, L., Jr. *J. Am. Chem. Soc.* **1995**, *117*, 3999−4013.
(8) Ha, E. H.; Ho, R. Y. N.; Kisiel, J. F.; Valentine, J. S. *Inorg. Chem.* **1995**, *34*, 2265−2266.
(9) San Filippo, J., Jr.; Chern, C. I.; Valentine, J. S. *J. Org. Chem.* **1976**, *41*, 1077−1078.
(10) San Filippo, J., Jr.; Romano, L. J.; Chern, C. I.; Valentine, J. S. *J. Org. Chem.* **1976**, *41*, 586−588.
(11) Hegg, E. L.; Ho, R. Y. N.; Que, L., Jr. *J. Am. Chem. Soc.* **1999**, *121*, 1972−1973.
(12) Mehn, M. P.; Fujisawa, K.; Hegg, E. L.; Que, L., Jr. *J. Am. Chem. Soc.* **2003**, *125*, 7828−7842.

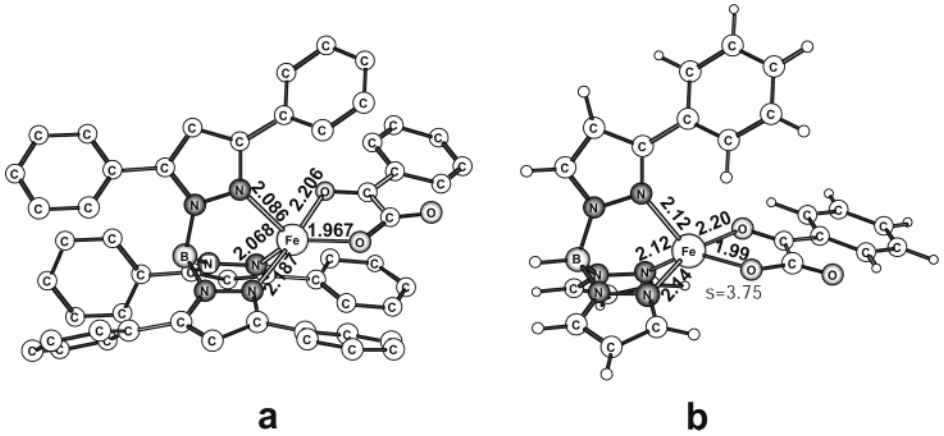

Figure 1. (a) Crystal structure of [Fe(Tp^{Ph2})BF] (**1**). (b) Computational model of **1** used in this study.

Besides the leading compound **1**, derivatives having various substituents at the phenyl ring of BF were examined. Kinetic measurements performed with these derivatives indicated that the Hammett parameter σ of the substituent correlates very well with the activity of a given compound. Because the reaction rate increases with electron-withdrawing groups, while electron-releasing substituents have an adverse effect on the rate, it was proposed that the rate-limiting step has nucleophilic character; for example, it could be a nucleophilic attack of iron(III)-bound $O_2^{\bullet-}$ on the α-keto carbon of BF.

Even though the biomimetic studies, summarized above, have provided firm evidence for the dioxygenase activity of **1** and very valuable thermodynamic and kinetic data, a more detailed picture of the reaction mechanism is desirable. More specifically, the spin state, relative energy, and chemical identity of transition states and intermediates on the reaction path leading to the final iron(III)−phenolate complex would provide a deeper insight into the mechanism of dioxygen activation and phenol ring oxidation. Such data would enable direct comparison with the recently published theoretical results on dioxygen activation in α-KG-dependent dioxygenases[13] and, therefore, reveal interesting analogies and differences between the mechanisms utilized by the enzymes and the biomimetic system. With this goal, a hybrid density functional study was performed for the biomimetic reaction mechanism. Since the computational approach adopted here is identical to the one used in our previous study modeling α-KG-dependent dioxygenases, direct comparisons are possible and should provide additional data concerning factors tuning the mechanism of dioxygen activation.

In the following subsection, the computational methods are described. Then, the results follow in the order of chemical steps on the reaction path. In general, good agreement between computational results and experimental data has been found. The rate-limiting nature of the dioxygen activation step has been confirmed, but the detailed mechanism of this process seems to be different in the enzymes and the biomimetic complex **1**. Finally, the identities of other transition states and intermediates have been resolved, which allows a mechanism of the entire biomimetic reaction to be proposed.

II. Computational Details

The crystal structure of **1** and its computational model employed in the present study are shown in Figure 1. To reduce the computational cost, five phenyl rings of the Tp^{Ph2} ligand were replaced by hydrogen atoms in the computational model. One phenyl group of the Tp^{Ph2} ligand is retained in the model to allow a study of the reaction between the Ph group and the activated dioxygen species. Some of the polarization influence of the discarded Ph groups on the reaction energetics should be captured by the solvation model employed here. In this continuum-dielectric solvent model, parameters devised for benzene were used, which should be adequate also for the Ph group.

All calculations were performed employing hybrid density functional theory (DFT) with the B3LYP[14,15] exchange-correlation functional. Two programs, Gaussian[16] and Jaguar,[17] were used. Geometry optimizations and molecular Hessian calculations were performed with a valence double-ζ basis set coupled with an effective core potential describing the innermost electrons on iron. This particular basis set is labeled lacvp in Jaguar. For the optimized structures, the electronic energy was computed with a bigger basis set of triple-ζ quality with polarization functions on all atoms (labeled lacv3p** in Jaguar). The solvent corrections were calculated with the self-consistent reaction field method implemented in Jaguar.[18,19] A dielectric constant of 2.3 with a probe radius of

(13) Borowski, T.; Bassan, A.; Siegbahn, P. E. M. *Chem. Eur. J.* **2004**, *10*, 1031−1041.

(14) Becke, A. D. J. *Chem. Phys.* **1993**, *98*, 5648−5652.
(15) Lee, C.; Yang, W.; Parr, R. G. *Phys. Rev.* **1988**, *B37*, 785−789.
(16) Frisch, M. J.; Trucks, G. W.; Schlegel, H. B.; Scuseria, G. E.; Robb, M. A.; Cheeseman, J. R.; Zakrzewski, V. G.; Montgomery, J. A., Jr.; Stratmann, R. E.; Burant, J. C.; Dapprich, S.; Millam, J. M.; Daniels, A. D.; Kudin, K. N.; Strain, M. C.; Farkas, O.; Tomasi, J.; Barone, V.; Cossi, M.; Cammi, R.; Mennucci, B.; Pomelli, C.; Adamo, C.; Clifford, S.; Ochterski, J.; Petersson, G. A.; Ayala, P. Y.; Cui, Q.; Morokuma, K.; Malick, D. K.; Rabuck, A. D.; Raghavachari, K.; Foresman, J. B.; Cioslowski, J.; Ortiz, J. V.; Stefanov, B. B.; Liu, G.; Liashenko, A.; Piskorz, P.; Komaromi, I.; Gomperts, R.; Martin, R. L.; Fox, D. J.; Keith, T.; Al-Laham, M. A.; Peng, C. Y.; Nanayakkara, A.; Gonzalez, C.; Challacombe, M.; Gill, P. M. W.; Johnson, B. G.; Chen, W.; Wong, M. W.; Andres, J. L.; Head-Gordon, M.; Replogle, E. S.; Pople, J. A. *Gaussian 98*; Gaussian, Inc.: Pittsburgh, PA, 1998.
(17) *JAGUAR 4.0*; Schrödinger, Inc.: Portland, OR, 2000.
(18) Tannor, D. J.; Marten, B.; Murphy, R.; Friesner, R. A.; Sitkoff, D.; Nicholls, A.; Ringnalda, M.; Goddard, W. A., III; Honig, B. *J. Am. Chem. Soc.* **1994**, *116*, 11875−11882.
(19) Marten, B.; Kim, K.; Cortis, C.; Friesner, R. A.; Murphy, R.; Ringnalda, M.; Sitkoff, D.; Honig, B. *J. Phys. Chem.* **1996**, *100*, 11775−11788.

Table 1. Relative Energies[a], Distances, and Spin Populations for the Optimized 1-Dioxygen Complexes

multiplicity/ type	ΔE [kcal/mol]	ΔG [kcal/mol]	ΔH [kcal/mol]	$-T\Delta S$ [kcal/mol]	Fe−O1 [Å]	Fe−O2 [Å]	O1−O2 [Å]	sFe	sO_2
septet/end-on	3.1	12.8	2.9	9.9	2.57	3.71	1.26	3.83	1.82
septet/side-on	1.2	12.8	2.0	10.8	2.24	2.33	1.32	3.90	1.67
quintet/end-on	7.1	18.3	7.9	10.4	2.04	3.02	1.29	3.80	−0.15
quintet/side-on	6.4	18.6	7.2	11.4	2.16	2.26	1.34	3.99	−0.48
triplet/end-on	2.3	12.3	3.3	9.0	2.28	3.14	1.26	3.65	−1.89

[a] With respect to the isolated reactants.

2.60 Å has been used since these values correspond to benzene. All transition-state optimizations and Hessian calculations were performed with Gaussian 98, and the thermal corrections were calculated for a temperature of 303.15 K. The reported energies are relative energies calculated with respect to the isolated reactants, **1** and dioxygen. As the Hessian calculations are computationally very demanding, thermal corrections were calculated only for the most important structures, e.g., those which lie on the reaction path before the rate-limiting decarboxylation step.

Since all calculations were performed within the unrestricted formalism (UB3LYP), the problem of spin contamination and its effect on the calculated energetics arises.[20] However, it turned out that the studied reaction proceeds almost exclusively on the septet potential energy surface, which is not affected by this phenomenon. Some of the quintet and triplet species were found to be spin contaminated, but still the calculated expectation values of the S^2 operator are within reasonable limits. The $<S^2>$ values, for the noninteracting Kohn−Sham system, calculated for all structures presented in this paper are reported in the Supporting Information.

Concerning spin populations and oxidation states of iron in complexes with typical N- or O-donating ligands, a simple correlation was noticed in this and many previous theoretical studies.[21−23] For the high-spin ($S = {}^5/_2$) iron(III) complexes, a spin population of about 4.0 is usually found on the metal, with the remaining spin density delocalized on the ligands. For the high-spin ($S = 2$) iron(II) complexes, the spin population on iron is usually in the range 3.7−3.8. When an iron(IV)−oxo moiety is present, the spin of the formally Fe(IV) ion is substantially delocalized onto the oxygen atom due to the covalent nature of the Fe−O bond; for the quintet Fe(IV)═O complexes, the spin population of about 3.0 is usually found on the metal. Therefore, the electronic structure of such a species is more easily interpreted in terms of the electronic configuration associated with the Fe═O double bond which resembles the electronic configuration of the triplet dioxygen.

III. Results and Discussion

A previous computational study of the dioxygen activation process in α-KG-dependent dioxygenases revealed that O_2 binding to the iron(II) active site leads to three species differing in spin state, but having similar energies.[13] Starting from these three possible iron−dioxygen complexes, septet, quintet, and triplet potential energy surfaces (PESs) were explored, and the stationary points along the reaction coordinate were localized. In summary, it was found that for the enzyme model the quintet PES involves the lowest barrier for the rate-determining step, i.e., the oxidative decarboxylation of α-KG. This step leads to an iron(II)−peracid complex, which then undergoes heterolytic O−O bond cleavage leading to the high-spin iron−oxo species. In contrast, on the septet PES, the process of dioxygen activation proceeds directly from the iron−dioxygen complex to the high-valent iron−oxo species. The septet transition state is located 6.4 kcal/mol higher than the quintet counterpart on the free-energy scale. The triplet PES involves an activation barrier twice as large as for the quintet potential energy surface, and therefore, it can be safely concluded that the triplet state does not participate in the process of O_2 activation.

In light of similarities between the first coordination shells of iron(II) in α-KG-dependent enzymes and **1**, it seems reasonable to assume that the dioxygen activation process will follow similar reaction paths. Indeed, comparable structures of the transition states and intermediates have been found for the O_2 activation process, but the relative energies are different in the enzyme and biomimetic systems. The results concerning this part of the biomimetic reaction, i.e., dioxygen activation, are discussed in the first four subsections below. More specifically, subsection 1 deals with the iron−dioxygen complex, while in subsection 2 the crucial oxidative decarboxylation of the cosubstrate is discussed. Subsections 3 and 4 are dedicated to the heterolytic O−O bond cleavage and the high-valent iron−oxo species, respectively. Subsections 5 and 6 describe the attack of the activated oxygen species, i.e., the high-valent iron−oxo complex, on the phenyl ring of the Tp^{Ph2} ligand, and the subsequent hydrogen shift, which completes the phenol fragment formation. The final oxidation of the iron(II)−phenol complex to the green iron(III)−phenolate compound is addressed in subsection 7.

1. Dioxygen Binding. The energy of isolated dioxygen and model **1** serves in this paper as a reference point for the biomimetic reaction. For this reason, it is natural that the structure of model **1** is discussed first. Crystal structures of the actual complex **1** and its computational model are displayed in Figure 1. In the present calculations, it has been found that the complex is in a high-spin state, e.g., quintet iron(II), which is consistent with NMR results obtained for **1**.[12] The alternative low-spin (singlet) and spin-intermediate (triplet) complexes have much higher energy than the quintet ground state, with the singlet lying 21.5 kcal/mol above the ground state. Therefore, only the high-spin state of **1** is accessible at ambient temperatures at which the biomimetic reaction of **1** was studied. As for the geometric structure, an overall good agreement between experimental X-ray and computational data can be recognized from the comparison

(20) Boone, A. J.; Chang, C. H.; Greene, S. N.; Herz, T.; Richards, N. G. J. *Coord. Chem. Rev.* **2003**, *238*−*239*, 291−314.
(21) Siegbahn, P. E. M. *Q. Rev. Biophys.* **2003**, *36*, 91−145.
(22) Blomberg, M. R. A.; Siegbahn, P. E. M. *J. Phys. Chem. B* **2001**, *105*, 9375−9386.
(23) Siegbahn, P. E. M.; Blomberg, M. R. A. *Chem. Rev.* **2000**, *100*, 421−437.

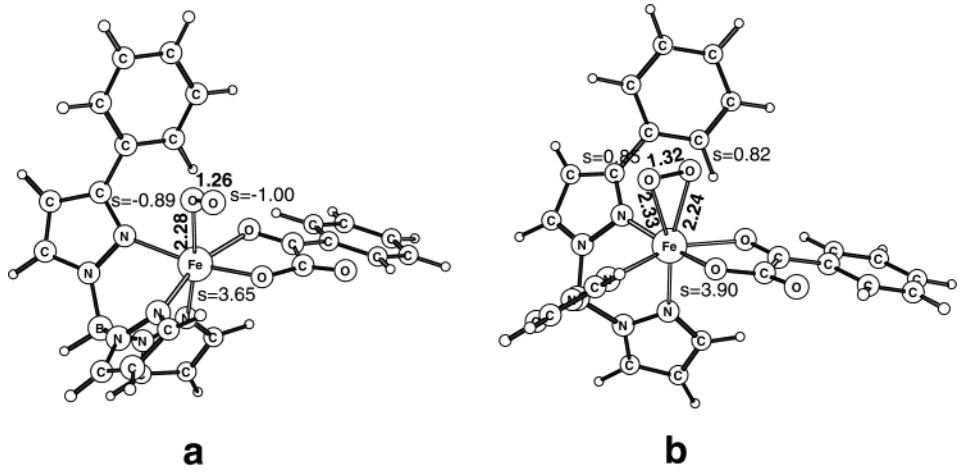

Figure 2. Optimized structures of (a) the triplet **1**−dioxygen complex and (b) the septet side-on **1**−dioxygen complex.

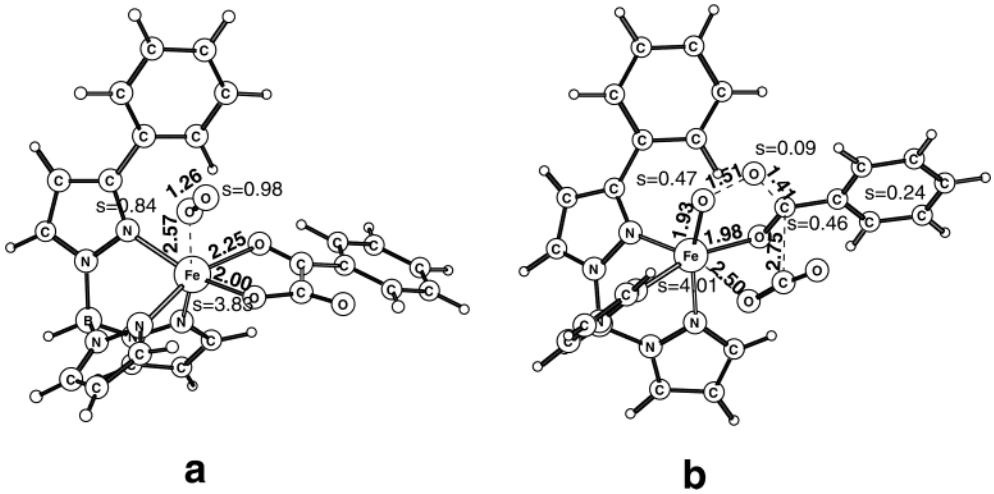

Figure 3. Optimized structures of the septet: (a) **1**−dioxygen complex and (b) transition state for oxidative decarboxylation of the keto acid.

of the bond lengths reported in Figure 1. The maximum deviation in bond lengths around iron does not exceed 0.05 Å, and the bidentate binding mode of BF is retained in the computational model. Having discussed the structure of **1** and its computational model, hereafter the latter will be denoted as **1** for the sake of clarity. Whenever the text refers to the actual [Fe(Tp^{Ph2})BF] complex, it will be explicitly mentioned.

Trapping of dioxygen by **1** leads to five different structures differing in spin and/or mode of O_2 binding. Besides the usually encountered end-on iron(II)−O_2 complexes in the septet, quintet, and triplet spin manifolds, side-on species turn out to be stable in the septet and quintet spin states. The most interesting bond lengths and contributions to the free energy of O_2 binding are collected for these species in Table 1, while the optimized structures of the two lowest energy complexes are depicted in Figure 2. Notably, the data reported in Table 1 indicate than in all five cases dioxygen binding is an endergonic process. While the enthalpy of O_2 trapping can be close to zero, the entropy term contributes at least 9 kcal/mol to the free energy of the **1**−dioxygen binding. It is interesting to note that the energies of O_2 binding calculated for the biomimetic end-on complexes follow those found for the enzyme model system.[13] In both cases, the triplet complex is the ground state, and the septet state has only slightly higher energy, while the quintet species is characterized by a markedly higher energy. In terms of electronic energy, the side-on binding mode stabilizes the septet **1**−O_2 complex with respect to the triplet end-on species, and this becomes the lowest energy structure. However, due to a slight difference in the entropies of side-on and end-on binding, the triplet end-on complex has lower free energy, and it is the ground state of the **1**−O_2 complex.

In the previous study, no dioxygen side-on binding structures, leading to 7-coordinated complexes, were found, and therefore, it is currently unclear if such species can form in the enzymatic system. This question will be addressed in a future study.

As regards the geometrical structure, dioxygen binding changes the coordination number of iron from 5 to 6 or 7, which means that the arrangement of the iron first shell ligands changes from distorted trigonal bipyramidal to distorted octahedral. Like the relative energies of the end-on complexes, the Fe−O and O−O bond lengths are very similar in the corresponding enzymatic and biomimetic structures. The only difference is that the septet **1**−O_2 complex has a long Fe−O bond (2.57 Å), while in the model of the enzyme active site this distance is only 2.28 Å. The different strengths of the Fe−dioxygen bonds in these septet complexes are manifested also in the O−O bond distances,

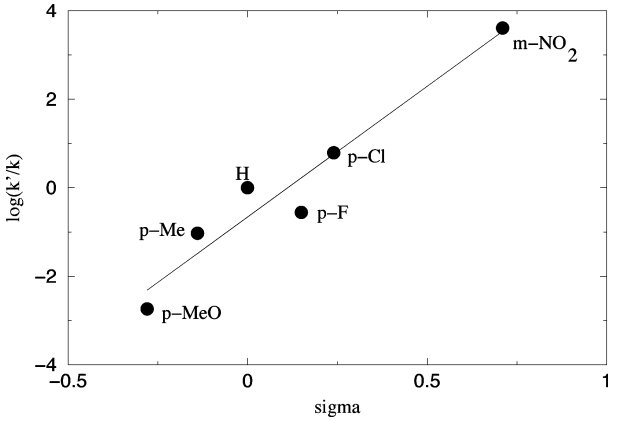

Figure 4. Hammett correlation plot for the calculated rates of the reaction between substituted **1** and dioxygen.

which are 1.26 and 1.31 Å in the synthetic and enzymatic systems, respectively. The origin of this difference is unclear, but one possible explanation could be different electron-donating capabilities of the first shell ligands. More specifically, a weaker electron-donating Tp^{Ph2} ligand, in comparison to the 2 His-1-carboxylate triad, would be less efficient in stabilizing iron(III), which is a component of the $Fe^{3+}-O_2^{\bullet-}$ adduct. Although the O−O bond lengths in the quintet end-on complexes seem to support this hypothesis (1.29 vs 1.34 Å in the biomimetic and enzymatic systems, respectively), it is only a tentative explanation for this quite small difference in properties of these two non-heme iron complexes.

2. Oxidative Decarboxylation. Starting from the structures of the end-on iron(II)−dioxygen complexes, septet, quintet, and triplet potential energy surfaces have been followed in search for stationary points along the oxidative decarboxylation path. In analogy to the results obtained for the enzyme model,[13] on the septet PES a single transition state connects the iron(II)−dioxygen complex with the septet high-valent iron−oxo species. This means that keto acid decarboxylation is concerted with O−O bond cleavage (for the transition state structure see Figure 3b). In contrast, on the quintet and triplet PESs, these two processes are sequential. The first transition state on these two potential energy surfaces leads from iron−dioxygen complexes to the iron(II)−peracid intermediate and carbon dioxide (the transition state structures are shown in Figure 5). In the subsequent step, heterolytic cleavage of the O−O bond in the peracid fragment leads to the high-valent iron−oxo species (intermediates and transition states for this process are presented in Figures 6−8). Interestingly, there is a minor difference between the biomimetic and enzyme model, as in the former there is no stable bicyclic triplet intermediate, while the latter forms such a structure.[13]

Because the results obtained in the current study indicate that the septet PES involves the lowest barrier for keto acid decarboxylation, the septet path is discussed first in this subsection. Then, the BF substituent effect on the reaction rate is described, while the results for the quintet and triplet PES are presented at the end of this subsection.

The optimized structures of the septet **1**−dioxygen complex and the transition state, leading to the septet hight-valent iron−oxo species, are depicted in Figure 3. A characteristic feature of this TS geometry, which was also encountered in the enzyme study,[13] is that it is a "late" TS as regards CO_2 release, but "early" TS with respect to O−O bond cleavage. Accordingly, the carbon−carbon bond length amounts to 2.75 Å, while the O−O distance equals only 1.51 Å. A notable difference between α-KG-dependent enzymes and the synthetic system studied here is seen in the spin distribution calculated for this TS geometry. In the biomimetic complex, the phenyl ring is bound directly to the critical carbonyl carbon which is involved in forming and breaking bonds at this step of the reaction. The total spin population of this phenyl fragment amounts to 0.24 for the TS geometry, which indicates a substantial delocalization of an unpaired electron onto this group. This spin delocalization, observed for the biomimetic complex, is most likely responsible for lowering the energy of the septet transition state with respect to the quintet counterpart (the quintet TS lies 8.8 kcal/mol above the septet TS; vide infra). In contrast, in α-KG-dependent enzymes an aliphatic side-chain takes the place of this phenyl ring, and as resonance delocalization is impossible in that case, for the enzyme model the septet TS was found 6.4 kcal/mol higher in free energy than the quintet one.[13] In the biomimetic system, the energetic order of these two transition states is reversed, with the septet TS lying 8.8 kcal/mol lower than the quintet counterpart. As this free energy difference (8.8 kcal/mol) is significant, it follows that the septet PES offers the most likely route for oxidative decarboxylation of the biomimetic cosubstrate, BF. At this point, it is also worthwhile to note that the concerted mechanism, in which an exergonic decarboxylation lowers the substantial barrier for O−O bond cleavage, was advocated in the literature concerning the biomimetic system.[11] Therefore, the results presented here and in the previous paper[13] indicate that this hypothesis, while not applying to α-KG-dependent enzymes, is in fact true for the biomimetic system.

As has already been discussed, the binding of O_2 to **1** is endergonic for all three multiplicities of the resulting **1**−O_2 species. Considering these data, the binary complexes seem to be unstable, and therefore, the activation energy for oxidative decarboxylation is calculated with respect to the isolated reactants, **1** and O_2. The thermodynamical data calculated for the septet TS compares favorably with available experimental data. The calculated $\Delta H^{\ddagger}$ is 10.0 kcal/mol, which should be compared with the experimental value of 6.0 kcal/mol, while the theoretical estimate of the entropy contribution ($-T\Delta S^{\ddagger}$) amounts to 11.3 kcal/mol, which matches well with the experimentally derived 12.8 kcal/mol. Summing these two contributions gives a free energy of activation amounting to 21.3 and 18.8 kcal/mol for the theoretical and experimental estimates, respectively. In conclusion, the activation enthalpy is overestimated by 4 kcal/mol, which is in the range of the usually assumed uncertainty of the methodology applied in this study. Finally, the underestimation of the entropy contribution by about 2 kcal/mol means that the two errors partially cancel, and the

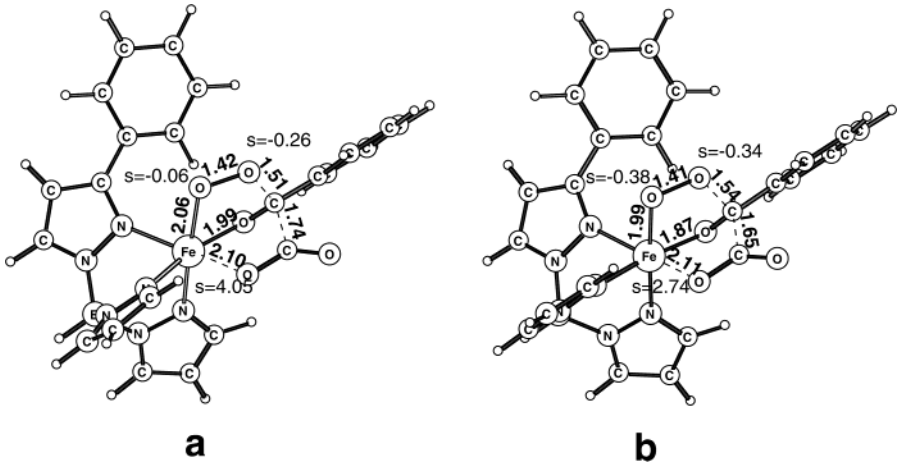

Figure 5. Optimized structures of the transition states for oxidative decarboxylation of the keto acid on (a) the quintet and (b) the triplet potential energy surfaces.

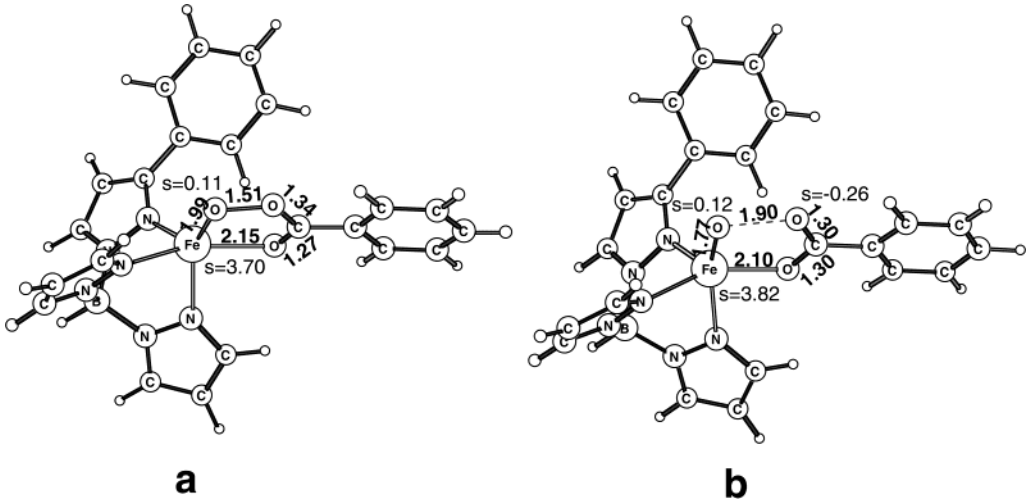

Figure 6. Optimized structures of the quintet: (a) iron(II)−peracid intermediate and (b) first transition state for O−O heterolysis.

calculated free energy of activation differs from the experimental value by only 2.5 kcal/mol.

The optimized structures of **1** and the septet transition state for oxidative decarboxylation have been used to assess the substituent effect on the barrier height. Due to the high computational cost for transition state optimizations and the general hypothesis that the PES is rather flat in TS regions, the following computational scheme has been adopted for studying the substituent effect. Models of the reactant and TS with an appropriate substituent at the phenyl ring of benzoylformate have been built from the optimized structures with unsubstituted BF. Subsequently, these structures have been relaxed in restrained optimization, where only the atoms of the substituted phenyl ring have been allowed to change their positions. The difference of the activation energy calculated for the substituted and unsubstituted complex **1** has been used as a correction to the calculated free energy of activation. These data enable the calculation of the logarithm of the relative rate constant, which is plotted as a function of the Hammett parameter σ in Figure 4. A positive slope and a high R^2 value (0.97) of this Hammett correlation plot agree very well with experimental data.[12] However, the substituent effect is exaggerated by the computational procedure used here, as the calculated slope parameter ρ is 5.9, while the experimental value is 1.3. The origin of this discrepancy remains unclear, but the tendency of calculations to exaggerate the substituent effects has already been reported in the literature.[24]

The quintet and triplet transition states for keto acid decarboxylation, shown in Figure 5, lie 8.8 and 18.4 kcal/mol higher than the septet counterpart on the free energy scale. Therefore, the calculated free energies of activation on the quintet and triplet PES (30.1 and 39.8 kcal/mol, respectively) seem to preclude these multiplicities from taking an active role in dioxygen activation in the biomimetic reaction. It is concluded that the septet path is the most likely route for the oxidative decarboxylation of **1**. Even though the quintet and triplet paths are found to be much less likely, the heterolytic O−O bond cleavage in the quintet and triplet iron(II)−peracid complexes is still described in the next subsection for the sake of comparison with the enzymatic system.

The geometric structures of the quintet and triplet TS are very similar to each other. The bond length of the C−C bond which is cleaved in this step is significantly shorter than in

(24) Himo, F.; Noodleman, L.; Blomberg, M. R. A.; Siegbahn, P. E. M. *J. Phys. Chem. A* **2002**, *106*, 8757−8761.

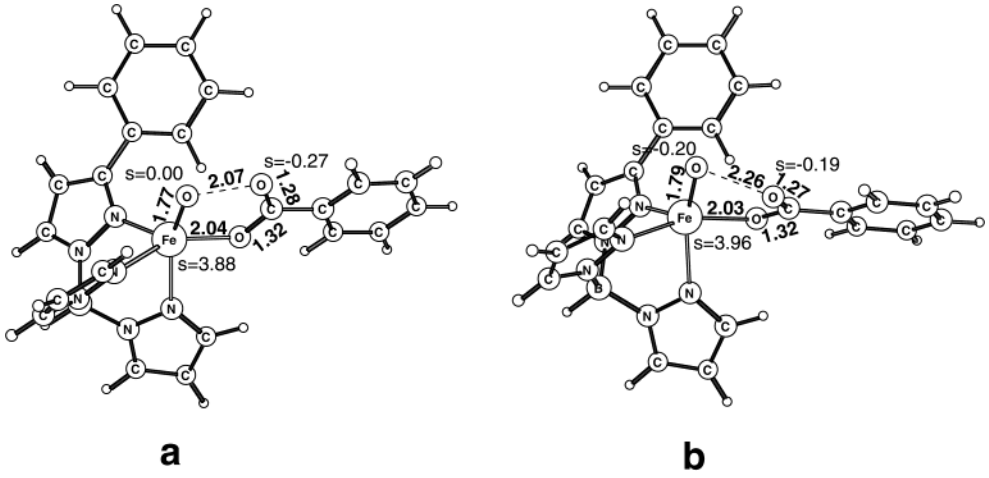

Figure 7. Optimized structures of the quintet: (a) intermediate with a partially broken O−O bond and (b) approximate second transition state for heterolytic O−O bond cleavage.

the septet transition state (see Figures 3 and 5). Similarly, the O−O distance in the quintet and triplet TS is around 0.1 Å shorter than in the septet transition state, which is consistent with the fact that this bond is retained in the quintet and triplet products of decarboxylation, i.e., the iron(II)−peracid complexes. Finally, the spin distribution is markedly different from the septet case, as there is no significant spin population on the reactant carbonyl carbon and the adjacent phenyl ring.

3. O−O Bond Cleavage in the Iron(II)−Peracid Intermediate. The quintet and triplet paths for dioxygen activation lead from the iron−dioxygen complex to the iron−peracid intermediate and carbon dioxide. Therefore, in order to get the high-valent iron−oxo species, the O−O bond in the peracid needs to be cleaved. In analogy to the enzyme system,[13] the heterolytic O−O bond cleavage takes place in two steps on the quintet PES, while in the triplet state only one transition state separates the iron(II)−peracid complex from the iron−oxo species.

The calculated energy of the quintet iron(II)−peracid complex, whose structure is depicted in Figure 6a, is −44.4 kcal/mol. This low value indicates that the decarboxylation reaction is irreversible at ambient temperatures. Stretching the O−O bond in this intermediate to 1.9 Å leads to a transition state which is 4.4 kcal/mol higher than the iron−peracid intermediate. While the O−O bond for this TS is 0.09 Å longer than in the corresponding enzymatic structure, the activation energy is similar to that calculated for the enzyme model ($\Delta H^{\ddagger} = 4.9$ kcal/mol).[13] Further analogies are found in the spin distribution. A comparison of the spin populations of the iron−peracid complex and this transition state indicates that one β-electron is being transferred from iron to the O−O bond. Passing the transition state leads to an intermediate with a partial bond between the two oxygen atoms, which was also found in the enzyme model study. A long O−O bond and the spin populations on the oxygen atoms in this structure, shown in Figure 7a, indicate a fractional bond order of the O−O bond. The calculated energy for this structure is −42.0 kcal/mol, which means that the first step of O−O bond cleavage is endothermic by 2.4 kcal/mol. Despite the fact that the first part of the heterolytic O−O bond cleavage is very similar in the biomimetic and enzymatic systems, the second TS for O−O bond heterolysis could not be found in the present study. However, in the enzyme model the activation energy for this second step amounts to only 0.5 kcal/mol, and vanishes completely when the solvent and thermal corrections are added.[13] Therefore, the activation energy calculated for the approximate TS, shown in Figure 7b, and amounting to about 2 kcal/mol, should not be far from the true value.

The calculated energy of the triplet iron(II)−peracid complex is −34.0 kcal/mol, which means that this species is 10.4 kcal/mol less stable than the quintet counterpart. The structure of this low-spin iron(II) complex and the transition state for its O−O bond cleavage is shown in Figure 8. The calculated energy of the latter structure is −32.6 kcal/mol, which indicates that the O−O bond cleavage on the triplet PES is very easy; the calculated activation barrier is only 1.4 kcal/mol.

4. High-Valent Iron−Oxo Species. As described in the two previous subsections, the oxidative decarboxylation of the keto acid cofactor together with CO_2 release and heterolysis of the O−O bond leads to the high-valent iron−oxo species, which like the iron−dioxygen complex can assume septet, quintet, or triplet multiplicities. The triplet and quintet species differ only in the pairing of the electrons occupying the nonbonding (δ) orbitals of the Fe═O core and, therefore, have similar Fe−O bond lengths and spin populations on oxygen (see Table 2). The difference between the electronic structure of the septet and quintet (triplet) species is more significant. The $\pi \rightarrow \sigma^*$ triplet excitation, which formally leads from the quintet to the septet species, results in a much longer Fe−O bond and a substantially larger spin population on oxygen (see Table 2). Therefore, the septet complex may be considered to have an $Fe^{III}-O^{-}$ core rather than the $Fe^{IV}=O^{2-}$.

The optimized structure of the quintet complex is presented in Figure 9, while the relative energies, most relevant bond lengths, and spin populations for the septet, quintet, and triplet iron−oxo species are collected in Table 2. In analogy to the enzymatic system, the quintet complex is computed to be the ground state. Moreover, the energetic gap between

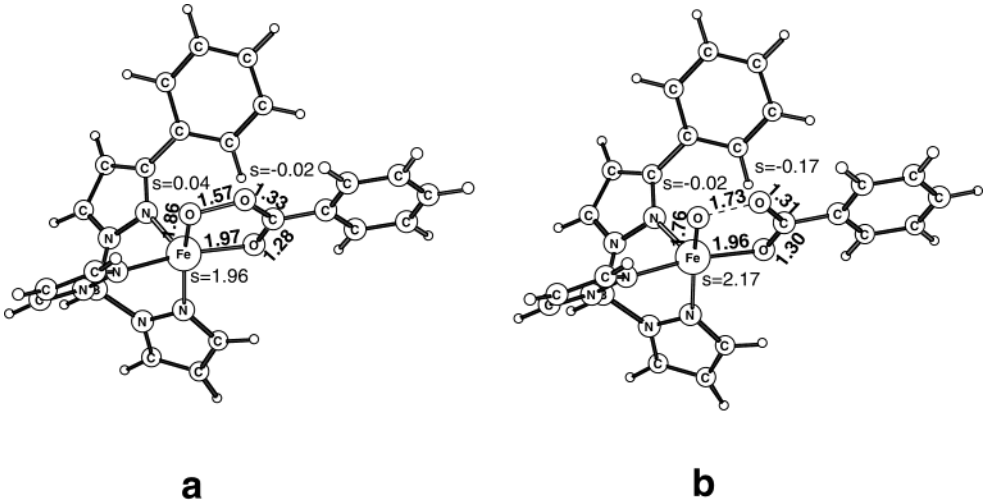

Figure 8. Optimized structures of the triplet: (a) iron(II)−peracid intermediate and (b) transition state for heterolytic O−O bond cleavage.

Table 2. Relative Energies, Bond Distances, Spin Distributions, and the Calculated $<S^2>$ Values for the Optimized High-Valent Iron−Oxo Species[a]

multiplicity	ΔE [kcal/mol]	Fe−O1 [Å]	Fe−O2 [Å]	Fe−O3 [Å]	sFe	sO	$<S^2>$
septet	−43.8 (17.1)	1.92	2.06	2.27	3.98	1.47	12.02
quintet	−60.9 (0.0)	1.65	2.07	2.26	2.90	0.83	6.05
triplet	−59.3 (1.6)	1.66	2.07	2.01	0.98	1.06	2.02

[a] O2 and O3 are carboxylate oxygens.

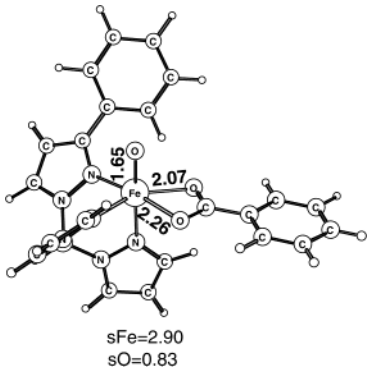

Figure 9. Optimized structure of the quintet high-valent iron−oxo species.

the quintet and septet states is similar to that calculated for the enzyme active site model (17.1 kcal/mol in the biomimetic system vs 13.4 kcal/mol in the enzyme). However, unlike in the previous study, the triplet species has only slightly higher energy than the ground state quintet. This difference can be attributed to the change of the carboxylate binding mode. In the case of the protein active site, arginine from the second coordination shell of iron is engaged in a strong hydrogen bond with one of the carboxyl oxygens. Therefore, only one carboxyl oxygen binds to iron resulting in a monodentate binding mode. In contrast, in the synthetic complex there are no basic groups nearby, and so benzoate binds to iron in a bidentate manner, which in turn should stabilize the triplet to a greater extent than the quintet state. Indeed, a comparison of iron−oxygen bond lengths in the quintet and triplet complexes supports this hypothesis (see Table 2). In the quintet complex one carboxylate oxygen is bound to iron more strongly than the other, with bond lengths of 2.07 and 2.26 Å. In the triplet species, the two iron−oxygen distances are almost equal (2.07 and 2.01 Å) and rather short. Therefore, from an energetic point of view the presence of the second carboxylate oxygen in the first coordination sphere of iron should be more crucial for the triplet state. The reactions between these iron−oxo species and the phenyl ring of the Tp^{Ph2} ligand are discussed in the next subsection.

5. Attack of the Activated Oxygen Species on the Phenyl Ring. The results discussed in the previous subsection indicate that the quintet and triplet states of the high-valent iron−oxo species have very similar energy. Both of these species can therefore participate in the phenyl ring oxidation. Moreover, even though the septet iron−oxo complex has been computed to be significantly less stable than the quintet and triplet ones, it is the septet iron−oxo species which is formed in the favorable decarboxylation route. Taking these observations into account, the reactions between all three iron−oxo species and the phenyl ring of Tp^{Ph2} ligand have been studied. Optimized structures of transition states and products of the electrophilic attack of the iron−oxo species on the phenyl ring are presented in Figure 10, while their energies together with spin and charge populations are gathered in Table 3.

The calculated activation energy on the septet potential surface is only 0.4 kcal/mol, which means that the septet iron−oxo complex can oxidize the phenyl ring very efficiently. A comparison of the spin populations on the iron−oxo fragment in the septet high-valent species and this transition state (Figures 9a and 10a) indicates that the spin on iron hardly changes during this reaction, while the spin on oxygen is significantly reduced.

The calculated activation energy on the quintet PES is lower than the experimentally estimated value for the whole process (18.7 kcal/mol), while on the triplet PES the calculated activation barrier exceeds this estimate slightly (see Table 3). However, since in the experiment no stable intermediate was observed during the whole reaction, the activation energies for processes other than oxidative decarboxylation should be on the order of 15 kcal/mol or less.

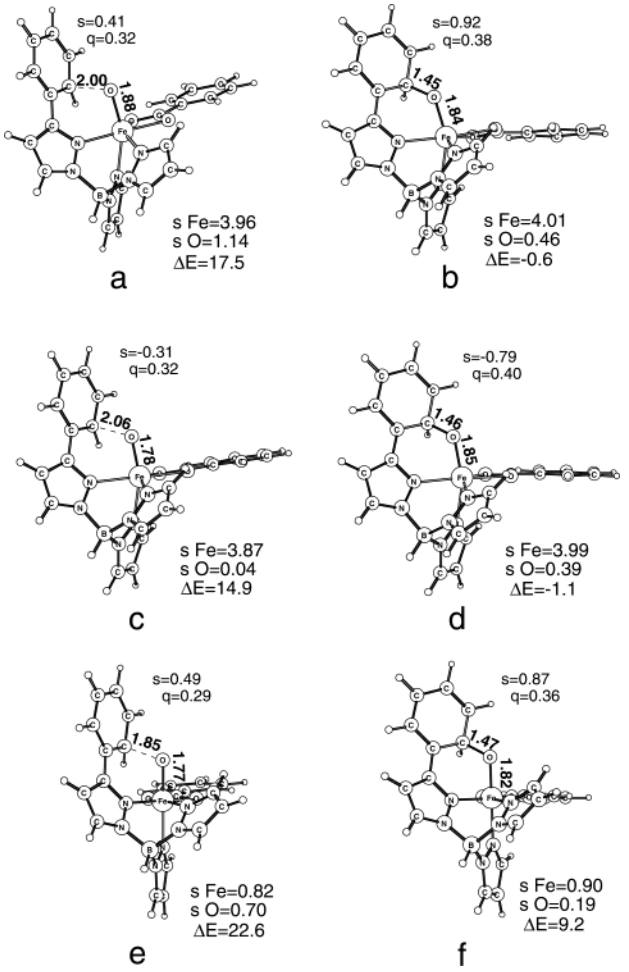

Figure 10. Optimized structures of transition states and products for electrophilic attack of the iron−oxo species on the phenyl ring: (a) septet TS, (b) septet product, (c) quintet TS, (d) quintet product, (e) triplet TS, and (f) triplet product. Relative energies [kcal/mol] are calculated with respect to the quintet iron−oxo species.

Table 3. Relative Energies, Activation Energies, and Spin and Charge Populations for the Optimized Transition States and Products of the Reaction between the High-Valent Iron−Oxo Species and the Phenyl Ring[a]

multiplicity/ species	ΔE [kcal/mol]	$\Delta E^{\ddagger}$ [kcal/mol]	spin on Fe	spin on Ph	charge on Ph
septet/TS	−43.4 (17.5)	0.4	3.96	0.41	0.32
quintet/TS	−46.0 (14.9)	14.9	3.87	−0.31	0.32
triplet/TS	−38.3 (22.6)	21.0	0.82	0.49	0.29
septet/product	−61.5 (−0.6)	-	4.01	0.92	0.38
quintet/product	−62.0 (−1.1)	-	3.99	−0.79	0.40
triplet/product	−51.7 (9.2)	-	0.90	0.87	0.36

[a] In parentheses, the relative energies with respect to the quintet iron−oxo species are given.

Taking into account this estimate and assuming an error bar of 3−5 kcal/mol for the methodology used in this study, both the quintet and triplet paths for phenyl ring oxidation seem to be viable. However, the experimentally observed lack of ^{18}O incorporation from labeled water into the product suggests a fast reaction between the iron−oxo species and the phenyl ring of the ligand.[12] Accordingly, the very low activation barrier on the septet PES indicates an efficient route for the phenyl ring oxidation which might explain the experimental findings of the isotope exchange.

As regards the products to which these transition states lead, in all three cases the phenol ring has been oxidized by one electron, as is evident from the spin and charge populations reported in Table 3. The absolute value of the spin accommodated on the Ph fragment amounts to at least 0.79, while the spin population on iron corresponds to either high-spin iron(III), in the case of septet and quintet products, or to low-spin iron(III), in the case of the triplet complex. The total charge on the Ph fragment is also more consistent with radical than cationic character of this part of the complex. Notably, the calculations undertaken for the quintet complex, with the hope to converge the electronic structure for iron(II) and the phenyl ring oxidized by two electrons, converged to an excited state with intermediate spin iron(III) and a one-electron oxidized phenyl ring. Therefore, these results seem to indicate that further structural rearrangements are necessary in order to obtain the two-electron oxidized phenyl ring. The greater stability of the iron(III)−$Ph^{\bullet}$ with respect to the iron(II)−Ph^{+} species originates most likely from the fact that the first shell ligands are negatively charged. Their total formal charge is −3, and it stabilizes the ferric oxidation state of iron. Because the coupling between the unpaired electrons on iron and the phenyl ring is weak, the septet and quintet complexes, which have high-spin iron, are almost degenerate and have very similar geometric structures. In contrast, in the triplet complex, which is 10.3 kcal/mol less stable than the ground state quintet, the iron−ligand bonds are significantly shorter, which is typical for low-spin complexes.

Finally, it is interesting to note at this point that very similar results for benzene oxidation by high-valent iron−oxo species were obtained in the model study of tetrahydrobiopterin-dependent hydroxylases.[25] Despite a different composition of the iron coordination shell and the fact that in the biomimetic system the "substrate" phenyl ring is a part of an iron ligand, transition state structures and energies are very similar in these two cases. Thus, this part of the biomimetic reaction establishes a link between α-keto acid- and tetrahydrobiopterin-dependent systems. Quite interestingly, a similar analogy was noticed for the dioxygen activation part of the catalytic cycle.[13]

6. Hydrogen Migration. In the previous subsection, it has been indicated that some structural rearrangement is necessary to promote the second electron transfer from the phenyl ring to iron. The most natural choice seems to be the transfer of the hydrogen atom, geminal to the oxygen bound to the ring, either to the adjacent carbon, or to the carboxyl oxygen of benzoate (see Figure 10d). The first possibility corresponds to the so-called NIH-shift and leads to a ketone, while the second one restores aromatic character of the ring and yields phenolate, the actual structure of the ring found in the final product of the biomimetic reaction. Notably, due to the strain induced by the bond between the phenyl ring and the Tp part of the Tp^{Ph2} ligand, a third possibility, which is arene oxide formation, seems very unlikely. Therefore, only the hydrogen migration has been addressed in the current study.

(25) Bassan, A.; Blomberg, M. R. A.; Siegbahn, P. E. M. *Chem. Eur. J.* **2003**, *9*, 4055−4067.

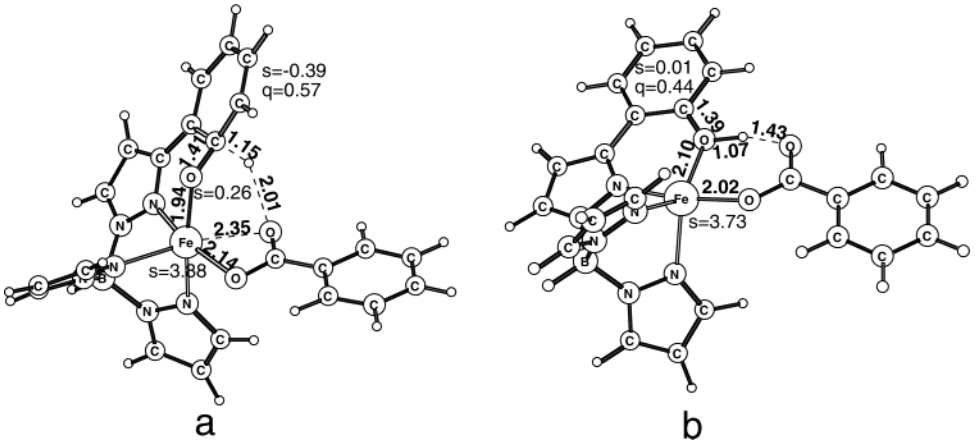

Figure 11. Optimized structure of the quintet: (a) transition state for proton-coupled electron transfer from the phenyl ring to iron, (b) iron(II)−phenol complex.

In addition, the septet and triplet species can be safely excluded from these investigations on the basis of simple electronic structure argument. Indeed, hydrogen atom migration is associated with an electron transfer from the phenyl ring to iron, which means reduction of iron(III) to iron(II) and quenching of the spin density on the phenyl ring. In the case of the septet and triplet complexes, this process leads to products in excited states, which most probably are at high energy. For this reason, the quintet path has been studied first, and because it involves a very low activation barrier, the septet and triplet PESs were not followed for this part of the biomimetic reaction.

The structures of the quintet transition state and the product for the proton-coupled electron transfer (PCET) reaction are presented in Figure 11. As has already been mentioned, in this process an electron is moved from the phenyl ring to iron, while a proton is transferred to the carboxylate oxygen of benzoate. The character of this process is best understood from the spin distribution. For the transition state (Figure 11a) the total spin population on the phenyl ring is reduced by half, when compared to the preceding structure (Figure 10d), while the hydrogen being transferred has a zero spin population. In addition, the spin population on iron is reduced monotonically in the series substrate (Figure 10d), to TS (Figure 11a), to product (Figure 11b), which further reinforces the proposed PCET mechanism. As for the barrier height, the calculated energy of the transition state is −60.1 kcal/mol, which means that the activation energy for this step is only 1.9 kcal/mol.

Once the transition state is passed, the proton migrates to the phenolate oxygen, as it is more basic than the carboxyl group. This means that the carboxylate oxygen plays a role of a "springboard" for the transferred proton, as no stable intermediate with hydrogen bound to this group could be located between the TS and the product. Quite interestingly, a similar role of a proton "springboard" was proposed for the porphyrin ligand in benzene oxidation catalyzed by cytochromes P450.[26] Therefore, a similar strategy for proton-transfer facilitated by an iron-bound base has been found for heme and non-heme iron systems.

(26) de Visser, S. P.; Shaik, S. *J. Am. Chem. Soc.* **2003**, *125*, 7413−7424.

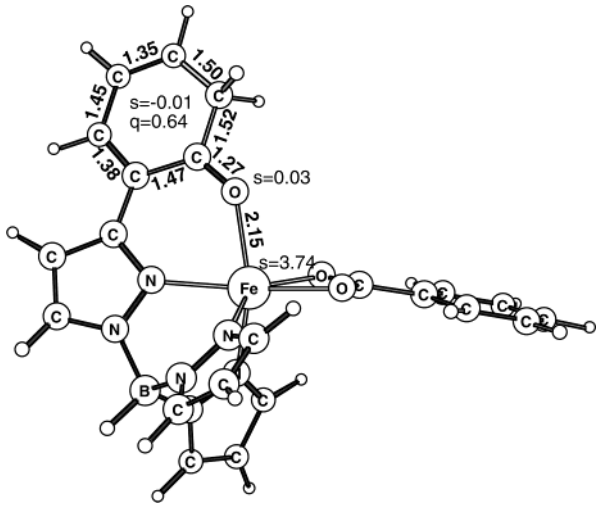

Figure 12. Optimized structure of the quintet iron(II)−ketone complex.

The structure of the product of this step, the iron(II)−phenol complex, is presented in Figure 11b. As regards the electronic structure, the spin populations on iron and the phenol ring indicate that the ring has been oxidized at the expense of the metal ion, which is now high-spin iron(II). As for the geometrical structure of this intermediate, the phenol proton is engaged in a strong hydrogen bond with the carboxyl group of benzoate, while the bond distance between the phenol OH group and iron has a value typical for iron(II) complexes. The calculated energy of this phenol−iron(II) structure is −119.0 kcal/mol, which renders the proton-coupled electron transfer exothermic by 57.0 kcal/mol.

The second possible route for the ring oxidation leads through a NIH-shift to an iron(II)−ketone product. However, despite many attempts, the transition state for this reaction could not be located because whenever the critical proton is moved from its equilibrium position, the carboxyl group approaches automatically. Therefore, it seems reasonable to assume that the electrostatic field produced by benzoate dominates the interactions of the migrating proton, and by this means its route. In the previous study on the tetrahydrobiopterin-dependent hydroxylases the barrier for the NIH-shift in the radical σ-complex was computed to amount to

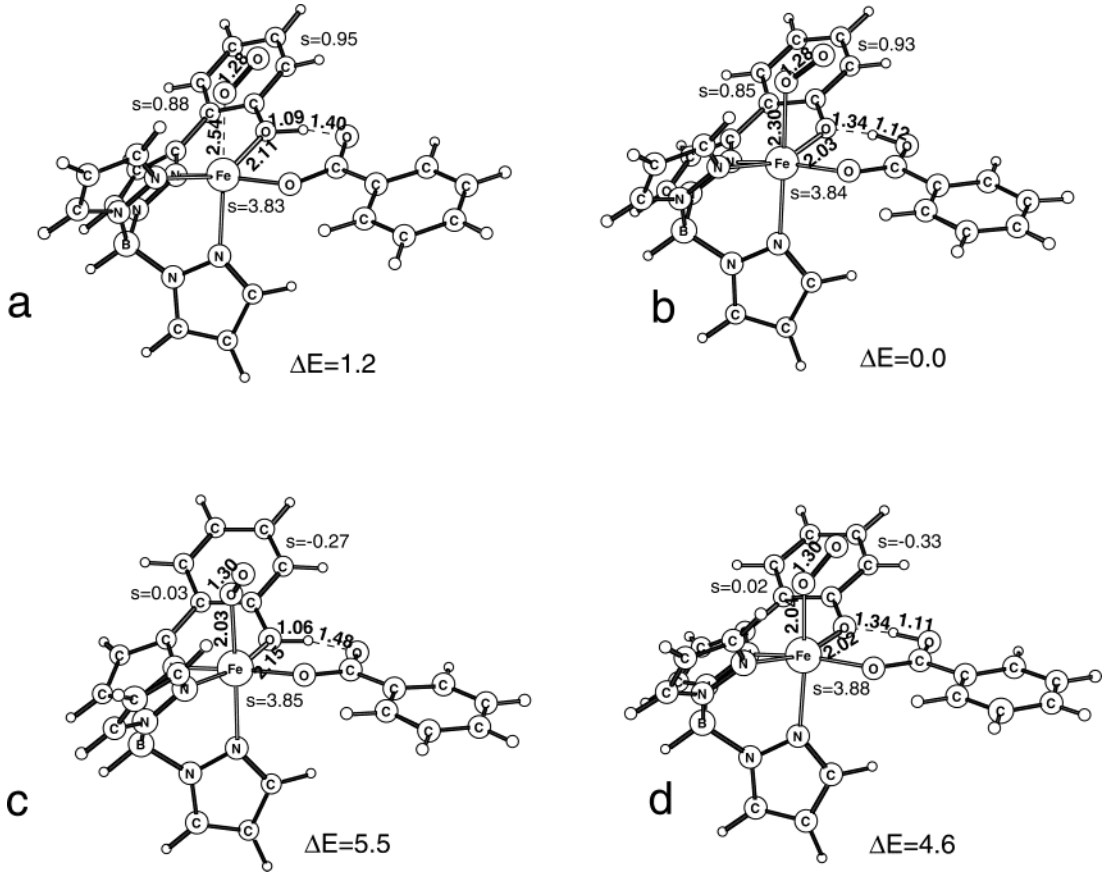

Figure 13. Optimized structures of two tautomeric forms of the phenol−iron(II)−dioxygen complexes: (a and b) septet, (c and d) quintet spin state. The relative energies are given in kcal/mol.

5.6 kcal/mol, which is three times larger than the barrier calculated here for proton-coupled electron transfer leading to the iron(II)−phenol complex.[25] Nevertheless, the product of the NIH-shift is a stable species, whose structure is shown in Figure 12. Like in the iron(II)−phenol complex, the spin populations on iron and the oxidized ring indicate a high-spin iron(II)−neutral ketone complex. This spin distribution is further corroborated by the bond lengths reported in Figure 12. The carbon−oxygen distance (1.27 Å) is typical for a carbonyl group, while the iron−oxygen bond is rather long (2.15 Å), as it should be for a weak iron(II)−carbonyl group interaction. The calculated energy of this hypothetical byproduct is −97.0 kcal/mol, which means that it is 22.0 kcal/mol less stable than the iron(II)−phenol complex. In light of this large energy difference between the two products for the proton migration, and the fact that the activation energy for the process leading to the more stable one is very low, it seems natural that the less stable product is not observed experimentally. The actual product of the two-electron phenyl ring oxidation, the iron(II)−phenol complex, is oxidized by dioxygen to the final iron(III)−phenolate product, and this process is discussed in the next subsection.

7. Fe(II) to Fe(III) Oxidation. One-electron oxidation of the iron(II)−phenol intermediate, which is performed by dioxygen, leads to an iron(III)−phenolate complex and a protonated superoxide radical. Since the high-spin (sextet) species of the iron(III)−phenolate complex was found to be the ground state and significantly more stable than the quartet and doublet species (by 10.6 and 9.8 kcal/mol, respectively), only those reaction pathways which can afford the sextet iron(III)−phenolate product have been considered in this study. Possible spin couplings of the unpaired electrons on the two products, i.e., the high-spin iron(III)−phenolate complex and $HO_2^{\bullet}$, lead to total quintet and septet spin states. Therefore, only on these two potential energy surfaces the products can be formed in their ground states, and for this reason, only septet and quintet paths have been studied for this final part of the biomimetic reaction.

Trapping of dioxygen by the iron(II)−phenol intermediate leads to adducts shown in Figure 13. In analogy to the first step of the biomimetic reaction, binding of dioxygen is endothermic by 3.2 and 7.1 kcal/mol for the septet and quintet spin states, respectively. Interestingly, once dioxygen is bound to iron, the second tautomer, in which benzoate is protonated, becomes stable (see Figure 13). The energies of these septet and quintet tautomers are about 1 kcal/mol lower than those calculated for the initial phenol−iron(II)−dioxygen adducts. Moreover, from the bond lengths reported in Figure 13 one can notice that the proton transfer from phenol to the carboxyl group affects the O_2 binding in the septet complex, since the iron−dioxygen bond shortens as the proton migrates. As regards the activation barrier of this tautomerization, initial potential energy scans indicate that the activation energy is lower than 3 kcal/mol. Due to this low value, no further effort was made to optimize the actual structures of the transition states. Once the proton is bound

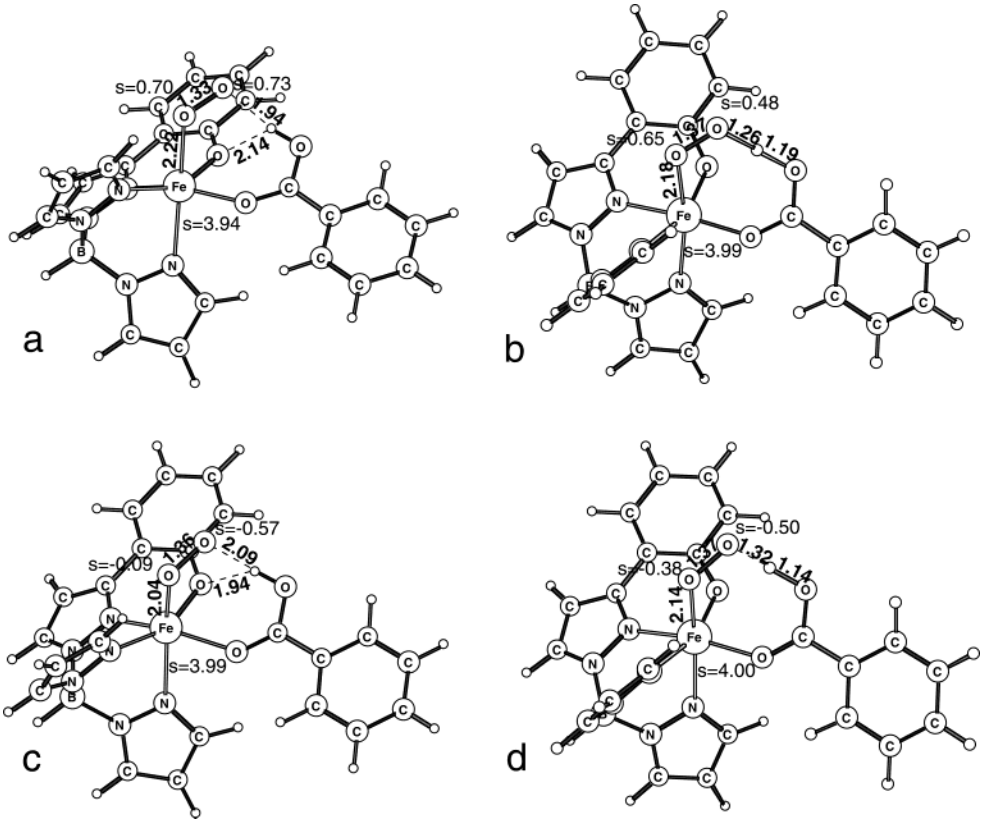

Figure 14. Optimized structures of transition states and products for the second intramolecular proton-coupled electron transfer: (a) septet TS, (b) septet product, (c) quintet TS, and (d) quintet product.

to the carboxyl group (see Figure 13b,d), the benzoate acts as a shuttle delivering the proton to form a hydrogen bond with the iron-bound dioxygen. Optimized transition states and products of this step are presented in Figure 14. The calculated activation energies are 2.8 and 6.5 kcal/mol for the quintet and septet spin states, respectively, while the absolute value of the reaction energy does not exceed 3 kcal/mol in these cases. Spin populations and bond lengths calculated for these products clearly indicate that the rearrangement of hydrogen bonds has been accompanied by electron transfer from iron to dioxygen. The spin population on iron, around 4 in both cases, is typical for high-spin iron(III) complexes, while the O−O distance of 1.37 Å and the total spin population on the dioxygen fragment (1.13 and −0.88 for the septet and quintet species, respectively) are characteristic for the superoxide ion. Starting from these two iron(III)−superoxide complexes and increasing the iron−oxygen distance, the final product of the biomimetic reaction, the iron(III)−phenolate complex, is obtained. On both potential energy surfaces, the septet and quintet, dissociation of the iron(III)−superoxide adduct leads to a monotonic energy increase along the reaction coordinate. The calculated reaction energy is 15.6 and 16.2 kcal/mol for the quintet and septet PES, respectively.

The optimized structure of the final product of the biomimetic reaction, the iron(III)−phenolate complex, is presented in Figure 15. The calculated bond length for the iron−phenolate oxygen bond (1.87 Å) compares very well with the crystallographic data obtained by Mehn and coworkers (1.888(1) Å). However, in the optimized structure

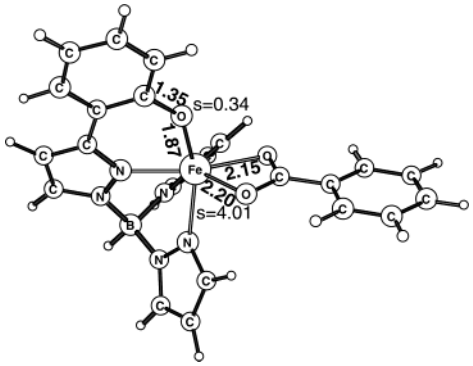

Figure 15. Optimized structure of the final product of the biomimetic reaction, the high-spin iron(III)−phenolate complex.

there is hardly any asymmetry in the iron−nitrogen bond lengths, while in the crystal structure one bond is about 0.14 Å shorter than the other two. This difference between the calculated and X-ray structures may have its origin in the fact that an extra molecule of 3,5-diphenylpyrazole is coordinated to iron(III) in the experimentally determined structure. Nevertheless, because the presence of this base is necessary only for obtaining crystals of the product, while the biomimetic reaction was studied in solutions deprived of it, this small structural difference does not undermine the computational results presented here.

Besides the iron(III)−phenolate complex, the $HO_2^{\bullet}$ radical is formed in 1-electron oxidation of the iron(II)−phenol complex by dioxygen. Once $HO_2^{\bullet}$ is released from the first coordination sphere of iron, it can dismutate to dioxygen and hydrogen peroxide. This process starts with binding two

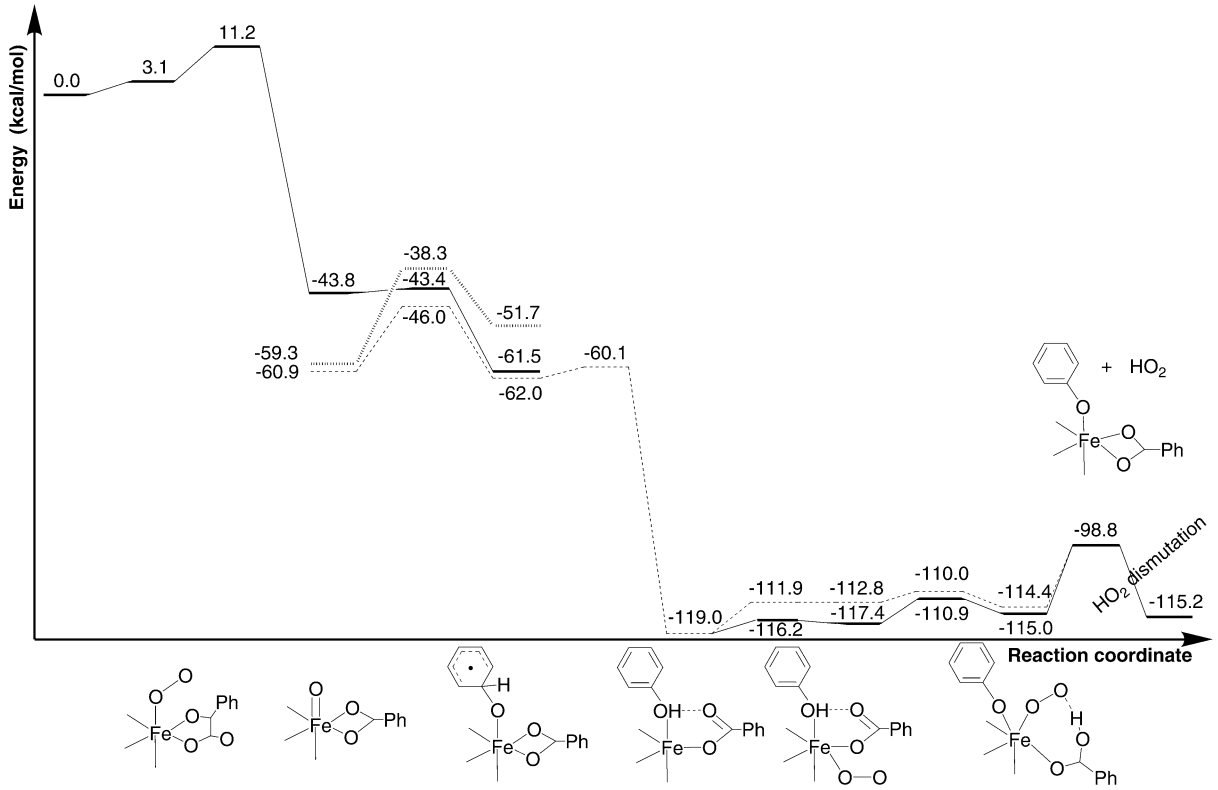

Figure 16. Electronic energy profile for the suggested mechanism of the biomimetic reaction: solid line, septet; dashed line, quintet; hashed line, triplet species.

molecules of $HO_2^{\bullet}$ by a hydrogen bond. The calculated association energy on the triplet PES is −6.3 kcal/mol. The transition state for proton-coupled electron transfer lies 2.4 kcal/mol below the energy of the separated reactants, which means that the activation energy is 3.9 kcal/mol. The product complex, which has an energy 32.9 kcal/mol lower than the isolated reactants, is composed of H_2O_2 very loosely bound to O_2. The whole dismutation reaction is exothermic by 32.8 kcal/mol, which combined with the low activation barrier indicates a fast and irreversible process.

IV. Conclusions

The results of the hybrid density functional calculations reported here indicate that the biomimetic reaction between **1** and dioxygen proceeds partially on the septet and partially on the quintet potential energy surface. Participation of the triplet species in the phenyl ring oxidation cannot be excluded, but is less likely. The calculated energy profile along the reaction coordinate is presented in Figure 16. In summary, the first irreversible step, which is dioxygen activation, proceeds most efficiently on the septet PES. The calculated free energy of activation for this reaction agrees well with experimental data and it is significantly lower than the barrier heights found for the quintet and triplet spin states. The calculated $\Delta H^{\ddagger}$ is 10.0 kcal/mol, and compares reasonably well with the experimental value of 6.0 kcal/mol, while the theoretical estimate of the entropy contribution ($-T\Delta S^{\ddagger}$) amounts to 11.3 kcal/mol, which matches well with the experimental value of 12.8 kcal/mol. Oxidative decarboxylation of BF coupled with O−O bond cleavage, which together constitute the dioxygen activation process, affords a high-valent iron−oxo species capable of oxidizing the phenyl ring of the Tp^{Ph2} ligand. As the iron−oxo species is formed in the septet state, and the quintet and triplet states lie at lower energy, several routes are available for the phenyl ring oxidation. First, the septet iron−oxo species can easily perform an electrophilic attack on the ring as the calculated activation energy for this step is only 0.4 kcal/mol. This efficient decay of the iron−oxo species agrees well with the lack of isotope exchange between the iron−oxo species and water. Second, a spin transition, which should be rather fast, leads from the septet to the quintet (or triplet) ground state iron−oxo species, which can subsequently oxidize the phenol ring, at a much lower rate than in the case of the septet PES, however. In either case, the iron−oxo species oxidizes the phenyl ring by 1 electron, which leads to a radical center on the ring. On the quintet PES, a transfer of the second electron from the ring to iron is promoted by proton transfer from the ring to the carboxyl oxygen of benzoate. Next, the resulting intermediate, the quintet iron(II)−phenol complex, binds dioxygen and tautomerizes to the iron(III)−superoxide species. Finally, protonated superoxide liberation yields the final product of the biomimetic reaction, the iron(III)−phenolate complex, while $HO_2^{\bullet}$ can easily dismutate to dioxygen and hydrogen peroxide.

Last, a short comment about the energy profile and the identity of the rate-limiting step follows. In Figure 16, two steps, oxidative decarboxylation of BF and release of $HO_2^{\bullet}$, have similar activation energies, and therefore, one might suspect that both of them control the overall reaction rate.

However, the activation entropies, having most probably comparable absolute values, have opposite sign for these two reactions. Oxidative decarboxylation involves dioxygen trapping, and therefore, the entropy term increases the activation barrier, while $HO_2^{\bullet}$ liberation enlarges the entropy, and for this reason the free energy barrier for this step is lowered by the entropy term. Taken together, the computational results reported here agree well with available experimental data and also provide additional insight into the molecular mechanism of this interesting biomimetic reaction. The latter should prove useful, for example, in the investigation of the catalytic mechanism of 4-hydroxyphenylpyruvate dioxygenase.

Supporting Information Available: Table S1 containing the calculated expectation values of the S^2 operator for all structures presented in the figures. This material is available free of charge via the Internet at http://pubs.acs.org.

IC035395C